# Viscoelastic Properties of Short Carbon Fiber Thermoplastic (SBS) Elastomer Composites

L. IBARRA,* A. MACÍAS, and E. PALMA

Instituto de Ciencia y Tecnología de Polímeros (C.S.I.C.), Juan de la Cierva 3, 28006 Madrid, Spain

SYNOPSIS

The determination of viscoelastic property variation in short fiber-reinforced composites, as a function of strain, temperature, and frequency, constitutes a useful tool when the existence or the strength of matrix–fiber interfaces are to be examined. In this work, these properties are studied in thermoplastic elastomer matrix materials (SBS) filled with commercial carbon fiber (PAN), oxidated, and subsequently treated with diazide, which generates $SO_2N_3$ groups on the fiber surface, theoretically capable of chemical reaction with the polymeric chain. For the composite containing diazide-treated oxidated fiber, certain phenomena have been proven to occur, such as lesser storing modulus losses in case of increasing strain, greater equivalent interfacial thickness values, and higher mechanical energy loss values than those of composite containing oxidated fiber. An increase in glass transition temperature and apparent activation energy of the relaxation process, with respect to composite-containing commercial fiber, are also observed, which, altogether, allow for the statement that new matrix–fiber bonds are generated through the sulfonyl azide group, conferring greater strength to the interface, although it is less stiff than the one formed with oxidated fiber. Finally, the experimental results are in agreement with those obtained from Huet's rheological model. © 1995 John Wiley & Sons, Inc.

## INTRODUCTION

In the manufacture of high-performance carbon fiber-reinforced polymers, good fiber–matrix adhesion is essential in order to ensure optimum stress transmission. Global interfacial interaction depends on specific chemical interactions and the occurrence of van der Waal's stresses among fiber and matrix surface atoms. The surface topography of the fiber, its roughness, porosity, etc., likewise contribute to interfacial adhesion by means of mechanical anchoring of the two components.

The surface reactivity of the carbon fibers can be improved by incorporating functional groups by means of an oxidative reaction, which will favor fiber–matrix interaction and facilitate potential chemical reaction with specific reagent groups. The mere elimination of low molecular weight carbon species, which are poorly bonded to the fiber surface, will improve the adhesion behavior of the fiber component.[1]

In elastomer reinforcement with a short fiber, the final $L/d$ ratio, i.e., the ratio existing after component treatment and blending, plays an important role in ensuring an adequate degree of reinforcement. In fact, the friction generated in the mixing chamber causes the fiber to deteriorate severely, which, to a greater or lesser extent, essentially depends on their flexibility. In this sense, carbon fibers, as well as glass fibers, undergo considerable mechanical degradation, and, hence, their final $L/d$ ratios approach the lower threshold of what is considered the optimum range.[2] This is probably the reason why conventional elastomer reinforcement with glass or carbon fiber has not been given any major development. This does, however, not apply to thermoplastic elastomers.

A thermoplastic elastomer is a material similar to rubber, showing the processing characteristics of conventional thermoplastics, as well as the prop-

* To whom correspondence should be addressed.

Journal of Applied Polymer Science, Vol. 57, 831–842 (1995)
 CCC 0021-8995/95/070831-12

erties of a conventional thermostable rubber.[3,4] Rubber materials generally contain a reinforcing agent: in most cases, carbon black. In thermoplastic elastomers, the polymer itself acts as a reinforcer, as a consequence of its composition and morphology.

Thermoplastic elastomers offer processing benefits, as compared to conventional thermostable rubbers, such as little or no blending, no need for curing, simpler processing and in fewer stages, as well as the possibility of recycling the material. Yet, they have the practical drawback of softening already at slightly elevated temperatures. This inherent property precludes their use in applications requiring temperatures approaching their softening point. Block copolymers of SBS, consisting of hard styrene segment and soft diene segment domains, are typical thermoplastic elastomers. As these elastomers present a composition similar to that of curable copolymers, except for their different macromolecular array, short-fiber reinforcement can be expected to improve their mechanical properties.

To test this hypothesis, in previous work,[5] mechanical property variation was studied in composites consisting of short carbon fiber and SBS matrix. The short fiber used was of the commercial type and treated according to a procedure by which functional reagent groups are incorporated into the fiber surface.[6] The mechanical properties obtained by means of fiber incorporation were consistently better than were those of the unfilled matrix, the higher property enhancement being observed for the diazide-treated samples, in spite of the deterioration undergone by the fibers during composite preparation.

The diazide treatment of the oxidated fibers is considered to be a good way to improve the composite properties. However, in the present study, the small differences between the mechanical behavior of the oxidated fibers composites and the diazide-treated oxidated fiber ones suggest that the level of modification is low.

In this work, the dynamic properties of these composites filled with commercial and treated carbon fiber are examined in terms of strain, temperature, and frequency, considering that these properties are less influenced by the $L/d$ ratio, as they refer to microscopic aspects of the material.

## EXPERIMENTAL

The experimental fiber is a carbon fiber based on polyacrylnitrile (PAN) cut to an approximate length of 6 mm and supplied by Hercules Aerospace España S.A. under the trade code 1815/AS with the following main characteristics: tensile strength, 2484 MPa; tensile module, 207 GPa; elongation at break, 1.2%; specific weight, 1.77; and filament diameter, 8 $\mu$m. The polymeric matrix consists of a 70/30 butadiene–styrene block copolymer, polymerized in solution, with a radial structure and supplied by Repsol Química S.A., under the trade name Calprene 416.

The oxidation method and subsequent treatment with 1,4-carboxysulfonyl diazide of the oxidated fiber were described in recent work.[6] An oxidated carbon fiber with a content of —COOH groups of 0.46 g/100 g fiber was used. The azide content of the treated fiber was 1.26 g/100 g fiber. The composite composition is as follows: Calprene 416 (SBS), 100; and carbon fiber, 10 vol per 100 parts by weight of polymer.

The surface characteristics of the commercial and the treated fibers, as measured by the BET method, as well as the aspect ratio of the fibers, before and after processing are compiled in the table below.

| Fiber | $S_{BET}$ ($m^2/g$) | Micropores ($cm^3/g$) | $L/d$ Before | $L/d$ After | Composite |
|---|---|---|---|---|---|
| Commercial | 0.27 | 0.058 | 859 | 46 | SBS–FC |
| Oxidated | 0.98 | 0.215 | 1055 | 43 | SBS–FCox |
| Azide-treated | 0.33 | 0.075 | 1078 | 42 | SBS–FCoxaz |

The viscoelastic properties of the polymeric matrix and the composites were measured in a Metravib viscoanalyzer RAC 815A, set at variable stress compression, strain, temperature, and frequency conditions.

## RESULTS AND DISCUSSION

### Variable Strain

The dynamic properties of elastomeric materials are a function of strain amplitude. Normally, they are

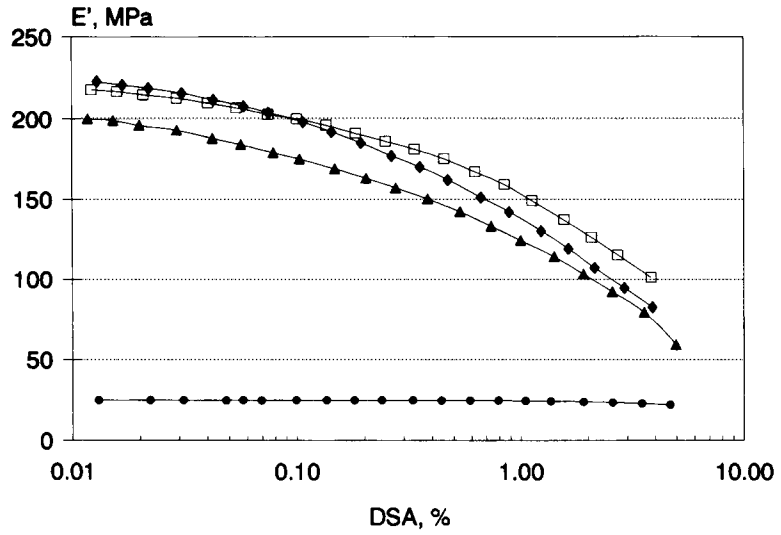


**Figure 1** Storage modulus $E'$ as a function of strain amplitude. Frequency 11 Hz, room temperature. Tension-compression test. Strain applied in longitudinal direction: (●) SBS matrix; (▲) SBS–FC; (♦) SBS–FCox; (□) SBS–FCoxaz.

independent of amplitude until the critical value is reached,[7] above which the modulus diminishes and the damping capacity (tan $\delta$ and the loss modulus $E''$) increases with amplitude. Occasionally, the dynamic mechanical properties tend to return to their original values, when the strain amplitude is reduced below its critical values. In the majority of cases, however, the modulus and damping do not regain their original values, which proves that some kind of permanent change has occurred in the polymer.

In the case of filled polymers, the changes in dynamic properties are caused by the rupture of filler agglomerates (in the case of particles) or by the breakage of filler–polymer bonds.[8]

Figure 1 shows the variation of the storage modulus $E'$ for the composites and the elastomeric matrix, as a function of strain amplitude, in terms of double-strain amplitude (DSA), when strain is applied longitudinally ($L$) to the preferential fiber orientation in the matrix. The curve corresponding to the polymeric matrix (SBS) is typical of an unfilled elastomer, where the modulus remains invariable vis-à-vis increasing strain. Fiber incorporation gives rise to a highly significant $E'$ increment, which gradually becomes smaller with increasing strain, yet without presenting any stretch of linear modulus response, i.e., the critical stress amplitude is extremely small. For high strain, the modulus value in any of the composites tends toward the value of the polymeric matrix.

When comparing the $E'$ values at low strain, the materials containing oxidated fiber (SBS–FCox) and diazide-treated oxidated fiber (SBS–FCoxaz) prove to possess a higher modulus value than that of the sample filled with commercial fiber. In principle, $E'$ is obviously influenced by fiber stiffness, and, hence, a substantial increase in stiffness is achieved with higher modulus values. Yet, there are also other factors with an effect on stiffness, such as polymer crosslink density, fiber interactions, and fiber–matrix interactions.

The composites under study have simple formulations: a polymer and a reinforcing agent. Therefore, the changes observed in material behav-

**Table I $E'$ Variation as a Function of the Strain Amplitude**

| Sample | $E'_0$ (MPa) | $E'_4$ (MPa) | $\Delta E'$ (MPa) | $E'_0/E'_4$ | $E'_{c,4}/E'_{m,4}$ |
|---|---|---|---|---|---|
| SBS | 24.9 | 22.5 | 2.39 | 1.106 | — |
| SBS–FC | 200 | 72.7 | 127.3 | 2.75 | 3.23 |
| SBS–FCox | 223 | 81 | 142 | 2.75 | 3.6 |
| SBS–FCoxaz | 218 | 98.5 | 119.5 | 2.21 | 4.38 |

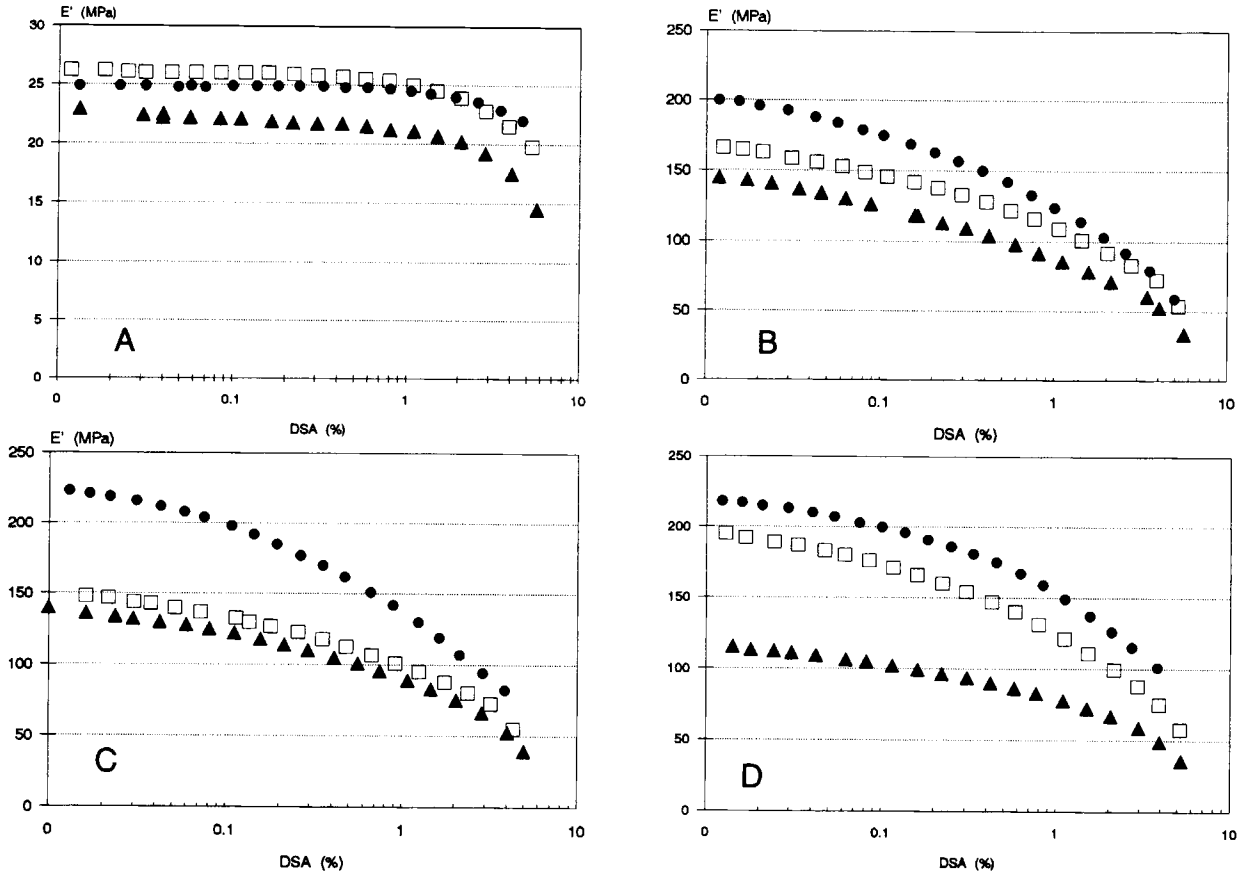


**Figure 2** Storage modulus $E'$ as a function of strain amplitude and testing temperature: (A) thermoplastic matrix; (B) SBS–FC composite; (C) SBS–FCox composite; (D) SBS–FCoxaz composite. (●) Room temperature; (□) 40°C; (▲) 60°C.

ior are exclusively due to the changes generated on the fiber surface. Table I shows the storage modulus values at minimum strain, $E'_0$, and at medium strain, $E'_4$, corresponding to a 4% strain in DSA, for the composites and the matrix.

With increasing strain amplitude, the fiber–fiber as well as the fiber–matrix bonds are gradually being destroyed. Hence, the more intense these interactions in the composite, the smaller the loss in the modulus. In this context, sample SBS–FCoxaz should be highlighted. It shows lower $\Delta E'$ and $E'_0/E'_4$ values and a higher $E'_{c,4}/E_{m,4}$ ratio, the latter which represents the effect of the fiber on the modulus value of the matrix, where $c$ and $m$ refer to the composite and the matrix, respectively. In the light of the data compiled in Table I, the sample containing oxidated and then diazide-treated fiber (SBS–FCoxaz) proves to produce a stronger interactions than does oxidated fiber (SBS–FCox), probably due to the presence of superficial $SO_2N_3$ groups capable of reacting with the polymeric chain.

In principle, the highest $E'_0$ modulus value corresponds to the oxidated fiber, which possesses COOH surface groups, a greater specific surface, and larger micropores, whereas at higher strain, these potential physical interaction sites disappear and the bonds generated by means of the sulfonyl azide group prove to be more stable.

Figure 2 shows the variation of the storage modulus as a function of strain amplitude (DSA) at different test temperatures. The modulus value of the thermoplastic matrix does not vary as the test temperature increases, from room to 40°C, but a decrease at any strain amplitude is observed when the test temperature was increased to 60°C, probably due to a softening of the hard polystyrene segments in the matrix [Fig. 2(A)].

Independent of fiber treatment, an increase in test temperature produces a diminution in modulus

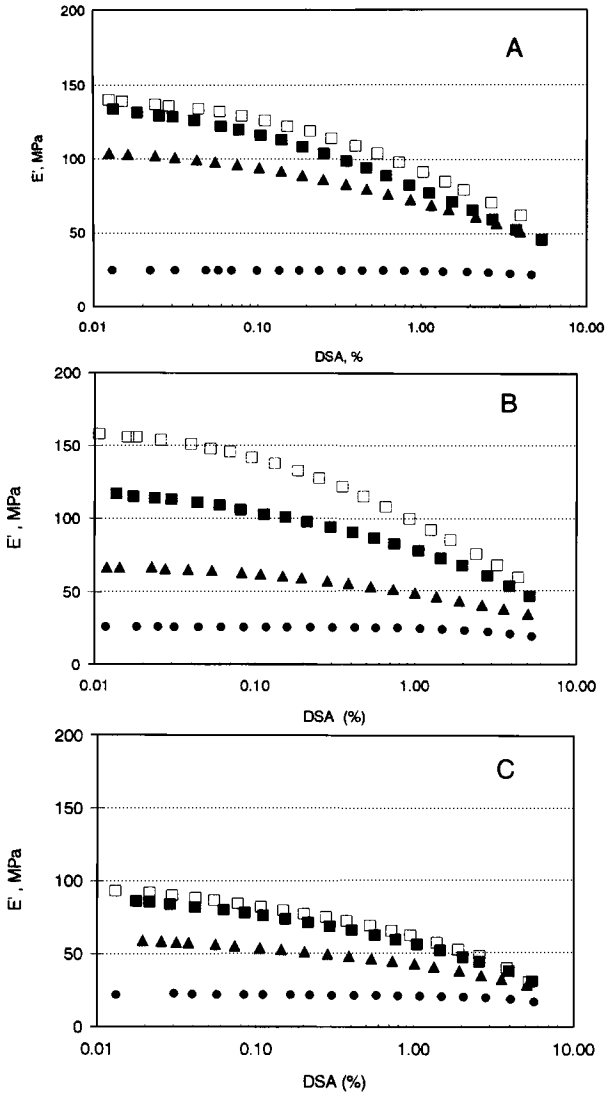


**Figure 3** Storage modulus $E'$ as a function of strain amplitude and testing temperature. Strain applied in transversal direction (T): (A) room temperature; (B) 40°C; (C) 60°C. (●) SBS matrix; (■) SBS–FC composite; (▲) SBS–FCox composite; (□) SBS–FCoxaz composite.

values of the composites. However, the oxidated fiber composite (SBS–FCox) showed a dramatic fall of the modulus at 40°C. At this temperature, the modulus value is very similar to those obtained at 60°C [Fig. 2(C)].

However, the decrease of the modulus of the diazide-modified oxidated fiber composite (SBS–FCoxaz) at 40°C is less marked than are those of the other composites, including the commercial fiber one. At this temperature, the modulus of the composite, at any strain amplitude, is the highest. However, at 60°C, a marked diminution of the modulus takes place, probably due to the damage of all matrix–fiber bonds. In this case, the shape of the curve is different, showing smaller decreases of the modulus as strain increases.

When strain is applied transversally (T) to the preferential fiber orientation (Fig. 3), the original modulus values are lower than are those obtained from longitudinal measurements (L), as a consequence of the anisotropy induced by the presence of the fibers. In addition, the shape of the curves varies also, showing less drastic modulus drops. On the other hand, at room temperature, it must be underlined that, at any strain, the highest modulus values are the ones obtained for the sample containing oxidated and diazide-treated fiber (SBS–FCoxaz).

The same pattern was observed at higher test temperatures, as shown in Figure 3(B) and (C), corresponding to 40 and 60°C, respectively, which shows that the modulus diminishes as testing temperature increases. In all cases, the modulus of the SBS–FCoxaz composite was higher than that of the others.

Dynamic property measurement as a function of transversally applied strain also allows one to determine the equivalent interfacial thickness, $\Delta R$, a new concept proposed to evaluate interfacial adhesion quantitatively,[9] expressed as

$$\Delta R = R_0(\sqrt{B - 1})$$

The higher the $\Delta R$ value is, the stronger the interfacial action is, and, thus,

$$B \cdot V_f = (E'_{c,T}/E'_{m,T}) - 1/(E'_{c,T}/E'_{m,T}) + 2$$

where $R_0$ is the fiber radius (average value used, 3.6 $\mu$m), and $V_f$, the fiber volume fraction in the material, and the subscripts $c$ and $m$ refer to the composite and the matrix, respectively.

The $E_T$, $B$, and $\Delta R$ values are listed in Table II, as calculated for two strains, at room temperature. At low strain, the differences between $\Delta R$ are small, although the highest absolute value corresponds to SBS–FCoxaz. When increasing the strain amplitude, the differences also increase, the SBS–FCoxaz sample again showing the highest value. In the last column, the respective equivalent interfacial thicknesses are shown for the two strain amplitudes, the sample in question being singled out as the one with the least thickness loss, probably due to the fact that in this material the interfacial bonds are more stable.

**Table II Equivalent Interfacial Thickness as a Function of the Strain Amplitude**

| | DSA 0.01% | | | DSA 4% | | | |
|---|---|---|---|---|---|---|---|
| Sample | $E'_T$ (MPa) | $B$ | $\Delta R_1$ | $E'_T$ (MPa) | $B$ | $\Delta R_2$ | $\Delta R_2/\Delta R_1$ |
| SBS | 24.9 | — | — | 23.5 | — | — | — |
| SBS–FC | 133.6 | 6.97 | 8.79 | 51.25 | 3.32 | 5.48 | 0.62 |
| SBS–FCox | 104 | 6.05 | 8.09 | 51.2 | 3.32 | 5.48 | 0.68 |
| SBS–FCoxaz | 140 | 7.13 | 8.92 | 62.5 | 4.19 | 6.43 | 0.72 |

Table III shows the calculated $\Delta R$ value at different temperatures, at 0.01% DSA. As observed, there is a loss of equivalent interfacial thickness in the SBS–FCox composite when increasing the test temperature at 40°C and remains almost constant at 60°C. However, in the SBS–FCoxaz composite, $\Delta R$ does not vary at 40°C and only a small decrease is observed at 60°C. The calculated $\Delta R$ values justify the variation of the modulus in both strain directions.

Figure 4 shows tan $\delta$ variation as a function of amplitude. The highest tan $\delta$ values are associated to friction phenomena, which, in the case of the sample filled with oxidated and treated fiber (SBS–FCoxaz), are lower owing to the stronger interface, reinforced by the bonds with the superficial azide group. Weaker interfaces prove incapable of resisting any substantial strain without rupture.[10]

The viscous component of the modulus, loss modulus $E''$, is associated to the energy dissipated in the material and transformed into heat, in such a way that for higher $E''$ heat generation, or transformed energy, is proportionally higher. Thus, hysteresis, or the heat generated per strain cycle, is described in the following expression:

$$H = (\pi/4)(\mathrm{DSA}/100)^2 E''$$

Table IV compiles the $H$ values calculated for several strain amplitudes as a function of strain direction, L or T. It can be observed that the mechanical energy loss differentials increase with increasing strain, in such a way that, with 0.1% DSA, the values calculated for SBS–FCox and SBS–FCoxaz are significantly higher, especially when strain is applied longitudinally.

**Table III Equivalent Interfacial Thickness as a Function of Testing Temperature**

| | Room | 40°C | 60°C |
|---|---|---|---|
| SBS–FC | 8.79 | 8.43 | 7.39 |
| SBS–FCox | 8.09 | 6.46 | 6.01 |
| SBS–FCoxaz | 8.92 | 9.2 | 7.75 |

When there exists links between the phases, a shear effect is generated in the interphase which produces an increment in mechanical energy loss. When the interfacial link is lacking, the value of the energy losses is likewise higher than that of the polymer matrix, due to the fiber ends that act as stress raisers, thus contributing to mechanical energy loss.[11] When strain is applied transversally (T), for any strain, the highest energy values refer to the composite containing oxidated and azide-treated fiber (SBS–FCoxaz).

## Variable Temperature and Frequency

Figure 5 shows storage modulus variation ($E'$) as a function of temperature at constant frequency and strain amplitude for the SBS matrix and the composite filled with commercial fiber, measured in both directions, L and T. In general terms, the shapes of the curves are similar, although detailed analysis allows one to detect some differences between them.

Modulus variation with temperature presents two zones of abrupt modulus drops, which correspond to the respective relaxations in the polymeric matrix: At low temperature, the glass transition of the soft butadiene segments, on the one hand, and, on the other hand, at high temperature, the melting of the hard styrene segments. Both transitions are discretely differentiated in the relaxation spectrum of tan $\delta$ plotted against temperature (Fig. 5).

In the glass zone, the $E'$ values of the matrix and the commercial fiber composite are very close together, i.e., in this temperature range, the contribution deriving from fiber stiffness to the material modulus is minimal. When increasing the temperature, the abrupt drop of the matrix modulus is compensated by fiber stiffness, which dampens the

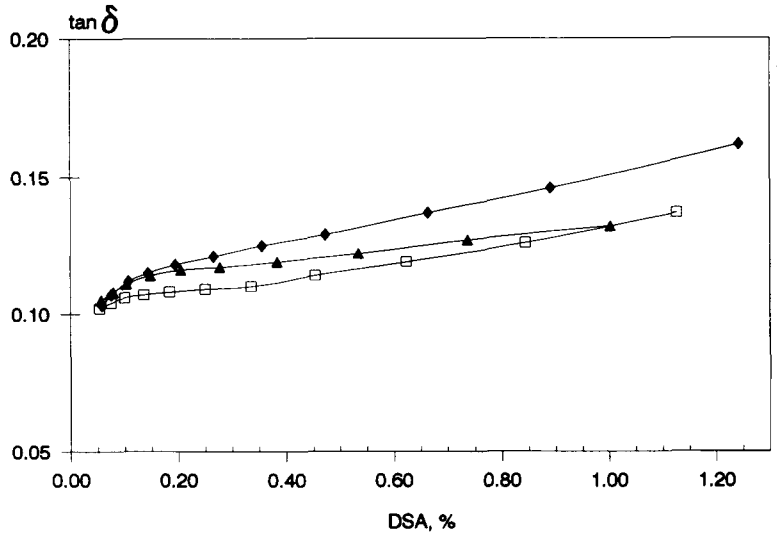


**Figure 4** tan $\delta$ as a function of strain amplitude in composite materials. Symbols as in Figure 1.

modulus drop in such a way that it is only noticeable in the elastic plateau zone, where the largest differences are produced. In addition, the effect of fiber orientation on the composite can be observed: When strain is applied transversal to the preferential fiber orientation, the modulus value is lower.

In the elastic plateau zone (−30 to 40°C), however, certain fluctuations of $E'$ are observed in the matrix, which are not present in the composite, where this zone shows relatively homogeneous values. This may be attributable to the existence of certain inhomogeneities in the interface between the hard and the soft segmental blocks, which become masked through fiber addition. These fluctuations are even more prominent in the than $\delta$ relaxation spectra.

The study of tan $\delta$ variation is an adequate method to detect the influence of any change occurring in any of the components of a composite material. Figure 6 shows this variation for the matrix and the commercial fiber composite, plotted against longitudinally and transversally applied strain. As

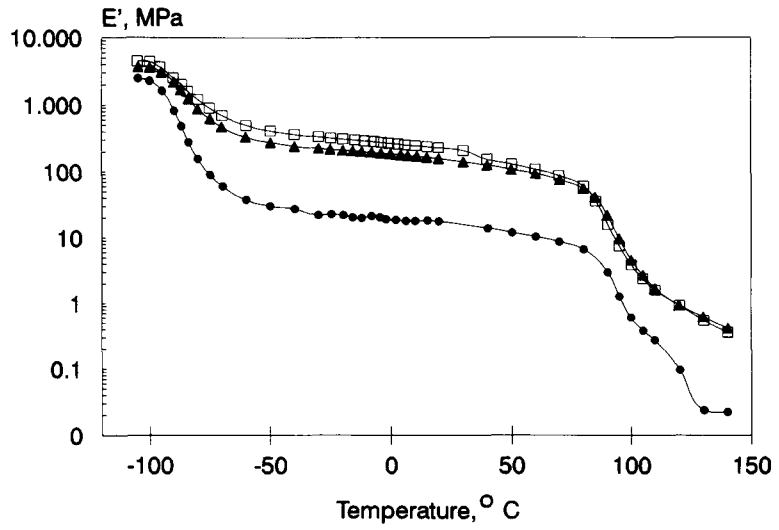


**Figure 5** Storage modulus, $E'$, as a function of temperature. Oscillation frequency 8 Hz. Strain amplitude 0.01% DSA. Tension-compression test. (●) SBS; (□) SBS–FC, strain applied in longitudinal direction; (▲) SBS–FC, strain applied in transversal direction.

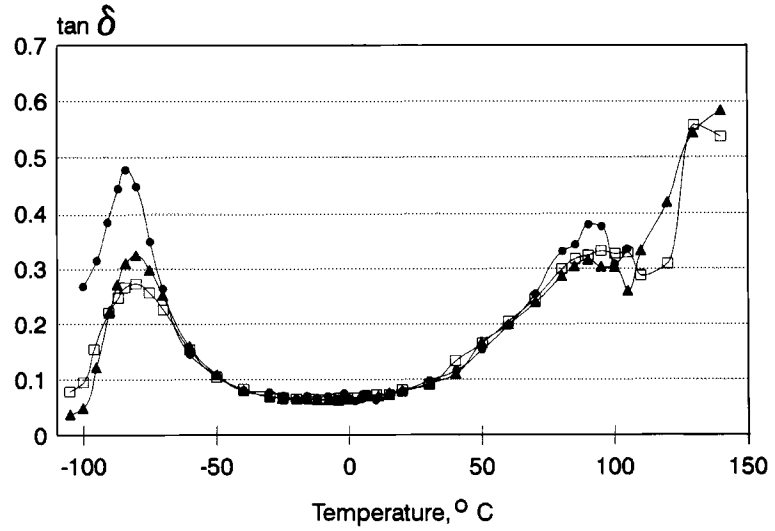


**Figure 6** tan $\delta$ as a function of temperature. Conditions and symbols as in Figure 5.

can be observed, the tan $\delta$ values of the composite are lower than are those of the matrix in the glass transition zone, the values obtained by means of transversal strain being situated between those corresponding to the matrix and the values obtained from longitudinal strain application. This situation can be explained by the fact that, when strain is applied parallel to the fibers, the greater stiffness of the fibers over the matrix causes the strain to be controlled by the fibers in such a way that the interface, which is assumed to be the more dissipative component in the composite, is strained to a lesser degree. This is why in our opinion it is preferable to consider the values obtained from transversal strain, as, here, the interface is easier to deform.

Table V shows the temperatures and amplitude of the tan $\delta_{max}$ peaks at different frequencies, the strain being applied perpendicular to the fiber direction. The incorporation of treated or untreated fiber reduces the amplitude of the tan $\delta_{max}$ peak, which remains practically invariable after surface treatment of the fiber. The only noteworthy changes occur in the temperature range of tan $\delta_{max}$. The most significant rise in the glass transition temperature of the matrix is recorded for the oxidated fiber sample (SBS–FCox), which, together with the decrease in amplitude, is to be attributed to an increment in interfacial stiffness achieved through more intense fiber–matrix interaction.[12] Oxidation eliminates the weakest cohesive surface layers from the fiber and enhances the concentration of functional groups, thus resulting in stronger matrix–fiber bonds and lesser molecular mobility in the interfacial zone. The replacement of functional groups by the diazide derivative gives rise to a drop in tan $\delta_{max}$ temperature, which, nevertheless, still remains above that obtained for commercial fiber, combined with a reduction in amplitude. This phenomenon could be

**Table IV Mechanical Energy Loss as a Function of the Strain Amplitude**

| | | DSA (%) | | | | | |
|---|---|---|---|---|---|---|---|
| Sample | Direction | 0.01 | 0.04 | 0.1 | 0.4 | 1 | 4 |
| SBS | | 0.014 | 0.235 | 1.49 | 24.3 | 153.9 | 2,513 |
| SBS–FC | L | 0.149 | 2.3 | 14.06 | 216.9 | 1323 | 20,415 |
| | T | 0.055 | 1.48 | 10.61 | 151 | 885 | 15,250 |
| SBS–FCox | L | 0.152 | 2.54 | 16.33 | 273.2 | 1759 | 29,453 |
| | T | 0.076 | 1.19 | 7.34 | 114.6 | 705 | 11,012 |
| SBS–FCoxaz | L | 0.152 | 2.52 | 16.09 | 266.1 | 1700 | 28,111 |
| | T | 0.103 | 1.64 | 10.23 | 163.1 | 1017 | 16,220 |

**Table V Tan $\delta_{max}$ Peak Characteristics as a Function of the Frequency**

| Sample | 5 Hz | 8 Hz | 12.5 Hz | 20 Hz |
|---|---|---|---|---|
| SBS | | | | |
| $T$ (°C) | −83.6 | −82.5 | −81.4 | −80.3 |
| Amplitude | 0.471 | 0.481 | 0.494 | 0.496 |
| SBS–FC | | | | |
| $T$ (°C) | −82 | −80.75 | −79.5 | −78.3 |
| Amplitude | 0.318 | 0.323 | 0.323 | 0.331 |
| SBS–FCox | | | | |
| $T$ (°C) | −79.3 | −78.2 | −77.1 | −76 |
| Amplitude | 0.333 | 0.341 | 0.344 | 0.346 |
| SBS–FCoxaz | | | | |
| $T$ (°C) | −81 | −80 | −79 | −77.9 |
| Amplitude | 0.317 | 0.325 | 0.332 | 0.340 |

explained in terms of a loss in interfacial stiffness and, hence, of a slight increase in molecular mobility.

When varying the vibration frequency of the spectra obtained, modulus $E'$, as well as tan $\delta$ variations, are similar in shape, although certain changes occur in the absolute values. The value of the modulus tends to increase with frequency at constant temperature. As to tan $\delta$, the temperature of tan $\delta_{max}$, which corresponds to the glass transition of the soft segment, is shifted to higher ranges as a result of higher frequency, thus increasing the amplitude of the peak, whereas the peak indicating the melting point of the hard segments diminishes in amplitude without causing any temperature shift.

According to Table V, any increase in vibrational frequency causes the glass transition temperature to rise and the amplitude of the damping peak to increase. The shift of the transition temperature allows one to calculate the apparent activation energy of the relaxation process for each of the samples, assuming a linear equation of the type

$$\log f = \log f_0 + \Delta E/2.303\ RT$$

By means of extrapolation, the glass transition temperature $T_{g,d}$ can be calculated, corresponding to a vibration frequency of 0.01 Hz, as shown in Table VI. The values listed in this table evidence increases in the glass transition and apparent activation energy for samples SBS–FCox and SBS–FCoxaz over SBS–FC. These changes have to be attributed to the lesser mobility in the polymeric chains,[13] due to

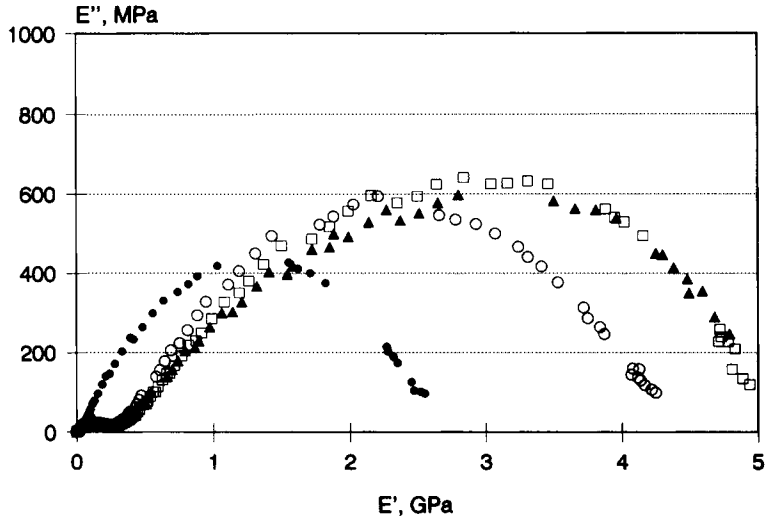


**Figure 7** Cole–Cole diagrams: (●) SBS; (▲) SBS–FC; (□) SBS–FCox; (○) SBS–FCoxaz.

the existence of stronger interfaces in these two composites. Yet, in light of the different $T_{g,d}$ and $\Delta E$ values in the composites filled with treated fiber, there must exist differences in interfacial composition deriving from the existence of azide group bonds in the sample SBS–FCoxaz.

## Cole–Cole Diagrams

There are instances in the literature where the changes in viscoelastic properties have been demonstrated by means of the Cole–Cole method, which had been developed for the study of dielectric dispersions. It was used, e.g., to examine the structural changes occurring in crosslinked polymers after fiber addition to polymeric matrices[14] or ligand addition to polymeric paint.[15]

The dynamic mechanical properties of these composites, when examined as a function of temperature and frequency, are represented on the Cole–Cole complex plane,[16] $E'' = f(E')$ (Fig. 7) show that (a) the experimental sites are positioned practically on a single curve, which means that the time–temperature superposition principle can be applied; (b) at high temperature (and low frequency), the graphs tend toward an asymptotic point $E'_0$, corresponding to the modulus of the relaxed material, and for low temperature (and high frequency), the graphs tend toward an asymptotic point $E'_\infty$, corresponding to the instantaneous modulus; and (c) the graph looks disymmetric.

According to the model developed by Huet,[17] angle $\beta$ at the origin is linked to a factor $h$ by means of the expression $\beta = h \cdot \pi/2$. By the same token, angle $\alpha$ at the other end is linked to a factor $k$ by means of the expression $\alpha = k \cdot \pi/2$. Hence, the experimental graphs can be described through an equation, such as the following:

$$E^* = E_0 + \frac{E_\infty - E_0}{1 + (i\tilde{\omega}\tau_1)^{-h} + (i\tilde{\omega}\tau_2)^{-k}}$$

where $\omega$ stands for frequency, $\tau_1$ and $\tau_2$ are the relaxation times ($\tau_1/\tau_2 = cte$), and $h$ and $k$ are the parameters corresponding to long and short times, respectively.

The values of $E_\infty$, $E'_0$, $\alpha$, $\beta$, $h$, and $k$ as calculated for the different samples with the fibers preferentially oriented in material flow direction (L), are compiled in Table VII(a). These values allow for the inference that, when carbon fiber is incorporated into the SBS matrix, the parameter characteristic of long relaxation times, i.e., $h$, diminishes. In contrast, $k$, the parameter indicative of short times, increases slightly and thus weakly constrains the movement of the molecular segments involved in relaxation. When analyzing the effects of fiber incorporation, $E'_0$ and $E'_\infty$ are not comparable.

For the sample filled with the oxidated fiber (SBS–FCox), $h$ increases vis-à-vis the value obtained for SBS–FC, which is indicative of the fact that in

**Table VI Apparent Activation Energies: Glass Transition Temperature**

| | $\Delta E$ (J/mol) | $T_{g,d}$ (°C) |
|---|---|---|
| SBS | 130.1 | −87 |
| SBS–FC | 117 | −86 |
| SBS–FCox | 129 | −83.3 |
| SBS–FCoxaz | 148 | −84.4 |

**Table VII Rheological Model Parameters for Composites**

| | $E'_0$ (MPa) | $E'_\infty$ (MPa) | $\beta$ | $\alpha$ | $h$ | $k$ |
|---|---|---|---|---|---|---|
| | | | (a) Longitudinal Measurements (L) | | | |
| SBS | 25 | 2730 | 37.7 | 25.5 | 0.42 | 0.283 |
| SBS–FC | 305 | 5280 | 22.8 | 26.6 | 0.25 | 0.295 |
| SBS–FCox | 355 | 5125 | 25.9 | 35.9 | 0.288 | 0.400 |
| SBS–FCoxaz | 290 | 4450 | 26.4 | 26 | 0.29 | 0.289 |
| | | | (b) Transversal Measurements (T) | | | |
| SBS | 25 | 2733 | 37.7 | 25.5 | 0.42 | 0.283 |
| SBS–FC | 208 | 4000 | 24.3 | 24.9 | 0.27 | 0.277 |
| SBS–FCox | 192 | 4150 | 25.5 | 26 | 0.28 | 0.289 |
| SBS–FCoxaz | 250 | 4865 | 25.9 | 19 | 0.29 | 0.215 |

one way or another the surface modification achieved has an impact on the network of the matrix. The simultaneous and substantial increment of $k$ evidences greater molecular segment constraint, which implies that the functional groups incorporated into the fiber surface and even the greater specific surface and microporosity of these fibers enhance fiber–matrix interaction. This, in principle, would harmonize with the higher $T_g$ value observed.

When treating the oxidated fiber with the diazide derivative, the increase of parameter $h$ is confirmed, but the simultaneous drop of $k$ signals a decrease in segmental blocking. These results are in good agreement with the findings reported in the literature for other matrices.[18]

The value of $E'_0$ increases upon fiber oxidation, but diminishes as a consequence of diazide treatment, which points toward the different nature of the interactions generated by the different fiber types. Although both surface modifications intervene in matrix crosslinking, the bonds resulting from the azide group are less rigid and give rise to a drop in the relaxed modulus. Yet, the rise in transition temperature in the diazide-treated sample, together with the increase in activation energy, as described above, indicate that there exists less mobility in the molecular segments of the matrix. When strain is applied transversally, the phenomena just described are less apparent, as shown by the similarity between the $h$ and $k$ values compiled in Table VII(b).

## CONCLUSIONS

The viscoelastic behavior of materials prepared with oxidated fiber (SBS–FCox) and with diazide-treated oxidated fiber (SBS–FCoxaz) presents variations which allow one to gain valuable insight into the characteristics of the matrix–fiber interface formed in the different composites.

When the viscoelastic properties $E'$ and tan $\delta$ are measured as a function of strain amplitude and at different testing temperatures, the results obtained support the statement that in materials containing diazide-treated and previously oxidated fiber (SBS–FCoxaz) a stronger interface is formed, as compared to composites filled with oxidated or commercial fiber. In fact, the smaller drop in the storage modulus, $\Delta E'$, and the lower tan $\delta$ values, together with their lesser dependence on strain increase, are indicative of the existence of an interface capable of resisting substantial strain without breaking. This finding is confirmed by the higher mechanical energy loss values and the greater equivalent interfacial thickness at any strain amplitude.

Different behavior of the interphase has been manifested by increasing the test temperature. In fact, the matrix–fiber interactions produced by treating oxidated fiber with a dizide derivative have proved to be less temperature-sensitive, at least between room temperature and 40°C. At any strain amplitude, the SBS–FCoxaz composite shows the highest moduli at 40°C.

The materials under study adjust to Huet's rheological model. The higher value of parameter $h$ in the SBS–FCoxaz sample vis-à-vis SBS–FC can be interpreted in terms of the effect exerted by the fiber–matrix bonds generated by the sulfonyl azide group, chemically bonded to the fiber surface. These diazide-induced bonds give rise to a less stiff interface, conferring greater mobility to the segments of the polymeric chain. In the case of oxidated fiber (SBS–FCox), the interface formed—presumably with the involvement of the oxygenated functional groups arising during fiber oxidation—is stiffer and exhibits less mobility, as can be inferred from the higher $k$ value.

On these same lines, the obtained results can be interpreted when measuring the viscoelastic properties as a function of temperature and frequency. In fact, the oxidated fiber confers greater stiffness to the interface, which produces greater immobility in the segments of the elastomeric chain, as the increase in glass transition temperature is greater than in the oxidated and diazide-treated fiber, which later, apart from producing the same immobilizing effect, causes a considerable increase in apparent activation energy of the relaxation process. From the different observed patterns, it is possible to infere that a new interphase was created by treating oxidated fiber with a diazide derivative.

The authors gratefully acknowledge the funding of this research by CICYT through the Project MAT 092/0917.

## REFERENCES

1. R. M. Bradley, X. Ling, I. Sutherland, and L. Davies, *J. Mater. Sci. Lett.*, **13**, 105 (1994).
2. K. Boustany and P. Hamed, *Rubber World,* **171**, 39 (1974).
3. M. W. Benjamin and Ch.P. Rader, *Handbook of Thermoplastic Elastomers,* Van Nostrand Reinhold, New York, 1988.

4. J. C. West and S. L. Cooper, *Science and Technology of Rubber,* F. R. Eirich, Ed., Academic Press, New York, 1978, Chap. 13.
5. L. Ibarra, A. Macías, and E. Palma, *Kauts. Gummi Kunstst.,* **48,** 180 (1995).
6. L. Ibarra and E. Palma, *Angew. Makromol. Chem.,* **220,** 111 (1994).
7. L. E. Nielsen, *Mechanical Properties of Polymers and Composites,* Marcel Decker, New York, Chap. 4.
8. A. I. Medalia, *Rubber Chem. Technol.,* **51,** 437 (1978).
9. Y. H. Zhou, T. Chen, W. D. Wu, C. Li, D. H. Li, and L. Q. Zhang, *Macromol. Rep.* **A30** (Suppl 5), 365 (1993).
10. J. Kubat, M. Rigdhal, and M. Welander, *J. Appl. Polym. Sci.,* **39,** 1577 (1990).
11. V. M. Murty, S. K. De, S. S. Bhagawan, R. Silvaramakrishana, and S. K. Athithan, *J. Appl. Polym. Sci.,* **28,** 3845 (1983).
12. P. Perret, J. F. Gérard, B. Chabert, A. Dartus, and J. Hognat, *Comptes-Rendus des Sixièmes Journées Nationales sur les Composites, JNC 6,* Paris, October 1988, Editions Pluralés, Paris, 1988, pp. 103–114.
13. M. Ashida, T. Noguchi, and S. Mashimo, *J. Appl. Polym. Sci.,* **30,** 1011 (1985).
14. B. Harris, O. G. Bradella, D. P. Hamed, C. Lefevre, and J. Verbert, *J. Mater. Sci.,* **28,** 3353 (1993).
15. B. Duperray, J. C. Laout, and J. L. Mansot, *Double Liaison Chim. Peint.,* **330,** 61 (1985).
16. K. S. Cole and R. H. Cole, *J. Chem. Phys.,* **9,** 341 (1941).
17. C. Huet, *Anal. Ponts Chaussées,* **6,** 373 (1965).
18. J. F. Gerard, *Polym. Eng. Sci.,* **28,** 508 (1988).

*Received August 8, 1994*
*Accepted February 19, 1995*